

Approximation of Functions on Manifolds in High Dimension from Noisy Scattered Data

Shira Faigenbaum-Golovin^{1,*} David Levin¹

¹ School of Mathematical Sciences, Tel Aviv University, Israel

* Corresponding author, E-mail address: alecsan1@post.tau.ac.il

December 29, 2020

Abstract

In this paper, we consider the fundamental problem of approximation of functions on a low-dimensional manifold embedded in a high-dimensional space, with noise affecting both in the data and values of the functions. Due to the curse of dimensionality, as well as to the presence of noise, the classical approximation methods applicable in low dimensions are less effective in the high-dimensional case. We propose a new approximation method that leverages the advantages of the Manifold Locally Optimal Projection (MLOP) method [14] and the strengths of the method of Radial Basis Functions (RBF) [13]. The method is parametrization free, requires no knowledge regarding the manifold's intrinsic dimension, can handle noise and outliers in both the function values and in the location of the data, and is applied directly in the high dimensions. We show that the complexity of the method is linear in the dimension of the manifold and squared-logarithmic in the dimension of the codomain of the function. Subsequently, we demonstrate the effectiveness of our approach by considering different manifold topologies and show the robustness of the method to various noise levels.

keywords: Manifold learning, Approximation of functions, High dimensions, Dimensional reduction, Noisy data

MSC classification: 65D99

(Numerical analysis - Numerical approximation and computational geometry)

1 Introduction

In this paper, we consider the following formulation of the problem of approximation of functions in a high-dimensional space. Let $f : \mathbb{R}^n \rightarrow \mathbb{R}^s$ be a function, and let $\{f(x_i)\}_{i=1}^K$ be its values on a given sample set of points $\{x_i\}_{i=1}^K \subset \mathbb{R}^n$ with noise present both in the domain of the function and in its codomain. The goal of the approximation is to estimate the values of the function at a new set of points. While in low dimensions numerous methods were suggested to solve this problem (e.g., splines, or Moving Least-Squares [18]), in high dimensions this is a challenging task due to the presence of noise and the curse of dimensionality. For instance, with respect to the latter challenge, if one merely assumes that the function is smooth, then approximation rates deteriorate severely with the growth of the dimension, the reason being

that the amount of sampled data should grow exponentially with respect to the dimension if one wishes to maintain the same order of approximation.

We categorize high-dimensional approximation methods according to whether the domain of the function to be approximated is a manifold or not. If no assumptions are made on the data domain, several methods were suggested. For example, solutions which treat non-smooth multivariate functions, [1], are based on sparse occupancy trees [5], Radial Basis Functions [13] (which we will discuss in detail below), or address the problem in the case where the values of the function lie on a manifold [16].

In many situations, the high-dimensional data reside on a low-dimensional manifold, and this information can be exploited to improve the approximation via one of the following two approaches: approximating in low dimension after dimension reduction, or alternatively approximating in high dimension. At times, reducing the dimension (e.g., in PCA [23], Multidimensional Scaling [11], Linear Discriminant Analysis [15], Locality Preserving Projections [17], Locally Linear Embedding [24], ISOMAP [27], Diffusion Maps [9], and Neural Networks in their general form, [21]) can lead to a better approximation (in terms of handling the challenge of the dimensionality, as well as the noise in the data). However, it may be non-efficient if the data volume is very large, and in addition, may result in information loss (due to some assumptions that need to be made on the data, e.g., regarding the data geometry, or the intrinsic dimension).

On the other hand, the assumption that the data reside on a manifold can be utilized to improve the approximation in high dimensions. Approximation of functions on manifolds is studied using local polynomials [4], wavelets [10], local linear regression [4], or neural networks [2,8,25]. For smooth functions on $[0, 1]^N$ which depend on a much smaller number l of variables, a solution was suggested in [12]. In addition, a recent paper, [26], proposed a solution based on Moving Least-Squares (MLS) that was designed to deal with noisy data with good rates of approximation.

In this paper, we propose a method of approximation of functions that leverages the advantages of the Manifold Locally Optimal Projection (MLOP) algorithm [14] to complement the strengths of the method of Radial Basis Functions (RBF) [6, 13]. We introduce this duet for approximation in high dimensions under noisy conditions (both in the domain and in the codomain of the function). In what follows we will provide a short introduction to the RBF method as well as to the Locally Weighted Average Approximation method (which will be used to contrast the RBF numerical results). In the next section, we will explain the proposed methodology, and demonstrate the improvement in approximation via several numerical examples.

2 Preliminaries

2.1 Preliminaries — the MLOP framework

The Locally Optimal Projection (LOP) method was introduced in [22] to approximate two-dimensional surfaces in \mathbb{R}^3 from point-set data. The procedure does not require the estimation of local normals and planes, or parametric representations. Its main advantage is that it performs well in the case of noisy samples. In [14] the LOP mechanism was generalized to devise the so-called *Manifold Locally Optimal Projection* (MLOP) method. Here, we give a concise overview of the MLOP method and its key properties.

First, we introduce the h - ρ condition, defined for scattered-data approximation of functions (which is an adaptation of the condition in [18] for low-dimensional data), to handle finite discrete data on manifolds.

Definition 1. h - ρ sets of fill distance h and density $\leq \rho$ with respect to a manifold \mathcal{M} . Let \mathcal{M} be a manifold in \mathbb{R}^n and consider sets of data points sampled from \mathcal{M} . We say that such a set $P = \{p_j\}_{j=1}^J$ is an h - ρ set if:

1. h is the fill distance, i.e., $h = \text{median}_{p_j \in P} \min_{p_i \in P \setminus \{p_j\}} \|p_i - p_j\|$.
2. $\#\{P \cap \bar{B}(y, kh)\} \leq \rho k^n$, $k \geq 1$, $y \in \mathbb{R}^n$.

Here $\#Y$ denotes the number of elements in a set Y and $\bar{B}(x, r)$ denotes the closed ball of radius r centered at x .

Note that the last condition regarding the point separation δ defined in [18], which states that there exists $\delta > 0$ such that $\|p_i - p_j\| \geq \delta$, $1 \leq i < j \leq J$, is redundant in the case of finite data. We also note that the vanilla definition of the fill distance uses the supremum \sup in its expression; here we use the median in order to deal with the presence of outliers.

The setting of the high-dimensional reconstruction problem is the following: Let \mathcal{M} be a manifold in \mathbb{R}^n of unknown intrinsic dimension $d \ll n$. There is given a noisy point-cloud $P = \{p_j\}_{j=1}^J \subset \mathbb{R}^n$ situated near the manifold \mathcal{M} such that P is a h - ρ set. We wish to find a new point-set $Q = \{q_i\}_{i=1}^I \subset \mathbb{R}^n$ which will serve as a noise-free approximation of \mathcal{M} . We seek a solution in the form of a new, quasi-uniformly distributed point-set Q that will replace the given data P and provide a noise-free approximation of \mathcal{M} . This is achieved by leveraging the well-studied weighted L_1 -median [28] used in the LOP algorithm and requiring a quasi-uniform distribution of points $q_i \in Q$. These ideas are encoded by the cost function

$$G(Q) = E_1(P, Q) + \Lambda E_2(Q) = \sum_{q_i \in Q} \sum_{p_j \in P} \|q_i - p_j\|_{H_\epsilon} w_{i,j} + \sum_{q_i \in Q} \lambda_i \sum_{q_{i'} \in Q \setminus \{q_i\}} \eta(\|q_i - q_{i'}\|) \hat{w}_{i,i'}, \quad (1)$$

where the weights $w_{i,j}$ are rapidly decreasing smooth functions. The MLOP implementation uses $w_{i,j} = \exp\{-\|q_i - p_j\|^2/h_1^2\}$ and $\hat{w}_{i,i'} = \exp\{-\|q_i - q_{i'}\|^2/h_2^2\}$. The L_1 -norm used in [22] is replaced by the “norm” $\|\cdot\|_{H_\epsilon}$ introduced in [19] as $\|v\|_{H_\epsilon} = \sqrt{v^2 + \epsilon}$, where $\epsilon > 0$ is a fixed parameter (in our case we take $\epsilon = 0.1$). As shown in [19], using $\|\cdot\|_{H_\epsilon}$ instead of $\|\cdot\|_1$ has the advantage that one works with a smooth cost function and outliers can be removed. In addition, h_1 and h_2 are the support size parameters of $w_{i,j}$ and $\hat{w}_{i,i'}$ which guarantee a sufficient amount of P or Q points for the reconstruction (for more details, see the subsection “Optimal Neighborhood Selection” in [14]). Also, $\eta(r)$ is a decreasing function such that $\eta(0) = \infty$; in our case we take $\eta(r) = \frac{1}{3r^3}$. Finally, $\{\lambda_i\}_{i=1}^I$ are constant balancing parameters.

In order to solve the problem with the cost function (1), we look for a point-set Q that minimizes $G(Q)$. The solution Q is found via the gradient descent iterations

$$q_{i'}^{(k+1)} = q_{i'}^{(k)} - \gamma_k \nabla G(q_{i'}^{(k)}), \quad i' = 1, \dots, I, \quad (2)$$

where the initial guess $\{q_i^{(0)}\}_{i=1}^I = Q^{(0)}$ consists of points sampled from P .

The gradient of G is

$$\nabla G(q_{i'}^{(k)}) = \sum_{j=1}^J (q_{i'}^{(k)} - p_j) \alpha_j^{i'} - \lambda_{i'} \sum_{\substack{i=1 \\ i \neq i'}}^I (q_{i'}^{(k)} - q_i^{(k)}) \beta_i^{i'}, \quad (3)$$

with the coefficients $\alpha_j^{i'}$ and $\beta_i^{i'}$ given by the formulas

$$\alpha_j^{i'} = \frac{w_{i,j}}{\|q_i - p_j\|_{H_\epsilon}} \left(1 - \frac{2}{h_1^2} \|q_i - p_j\|_{H_\epsilon}^2 \right) \quad (4)$$

and

$$\beta_i^{i'} = \frac{\widehat{w}_{i,i'}}{\|q_i - q_{i'}\|} \left(\left| \frac{\partial \eta(\|q_i - q_{i'}\|)}{\partial r} \right| + \frac{2\eta(\|q_i - q_{i'}\|)}{h_2^2} \|q_i - q_{i'}\| \right), \quad (5)$$

for $i = 1, \dots, I$, $i \neq i'$. In order to balance the two terms in $\nabla G(q_{i'}^{(k)})$, the factors $\lambda_{i'}$ are initialized in the first iteration as

$$\lambda_{i'} = - \frac{\left\| \sum_{j=1}^J (q_{i'}^{(k)} - p_j) \alpha_j^{i'} \right\|}{\left\| \sum_{i=1}^I (q_{i'}^{(k)} - q_i^{(k)}) \beta_i^{i'} \right\|}. \quad (6)$$

Balancing the contribution of the two terms is important in order to maintain equal influence of the attraction and repulsion forces in $G(Q)$. The step size in the direction of the gradient γ_k is calculated as indicated in [3]:

$$\gamma_k = \frac{\langle \Delta q_{i'}^{(k)}, \Delta G_{i'}^{(k)} \rangle}{\langle \Delta G_{i'}^{(k)}, \Delta G_{i'}^{(k)} \rangle}, \quad (7)$$

where $\Delta q_{i'}^{(k)} = q_{i'}^{(k)} - q_{i'}^{(k-1)}$ and $\Delta G_{i'}^{(k)} = \nabla G_{i'}^{(k)} - \nabla G_{i'}^{(k-1)}$.

Remark 2.1. The reasoning in terms of Euclidean distances, which is the cornerstone of the MLOP method, works well in low dimensions, e.g., for the reconstruction of surfaces in 3D, but breaks down in high dimensions once noise is present. To deal with this issue, a dimension reduction is performed via random linear sketching [29]. It should be emphasized that the dimension reduction procedure is utilized solely for the calculation of norms, and the manifold reconstruction is performed in the high-dimensional space. Thus, given a point $x \in \mathbb{R}^n$, we project it to a lower dimension $m \ll n$ using a random matrix, S , with certain properties. Subsequently, the norm of $\|S^t x\|$ will approximate $\|x\|$. The construction of S is carried out in the following steps:

1. Sample $G \in \mathbb{R}^{J \times m}$ with $G \sim N(0, 1)$.
2. Compute $B \in \mathbb{R}^{n \times m}$ as $B := P^t G$.
3. Calculate the QR decomposition of B as $B = SR$, and use S as the dimension reduction matrix.

Preliminaries — Optimal Neighborhood Selection

The support sizes h_1 and h_2 of the functions $w_{i,j} = \exp\{-\|q_i - p_j\|^2/h_1^2\}$ and $\widehat{w}_{i,i'} = \exp\{-\|q_i - q_{i'}\|^2/h_2^2\}$, respectively, are closely related to the fill distance of the P -points and the Q -points. Due to the importance of optimal selection of these parameters, we quote here several definitions and results from [14]. Unlike the standard definition of the notion of fill distance in scattered-data function approximation [18], we introduce

Definition 2. *The fill distance of the set P is*

$$h_0 = \text{median}_{p_i \in P} \min_{p_j \in P \setminus \{p_i\}} \|p_i - p_j\|. \quad (8)$$

Note that the vanilla definition of fill distance uses the supremum in the definition (instead of the median). However, as mentioned above, in our case we replace the supremum with the median so as to deal with the presence of outliers.

Definition 3. *Given two point-clouds, $P = \{p_j\}_{j=1}^J \subset \mathbb{R}^n$ and $Q = \{q_i\}_{i=1}^I \subset \mathbb{R}^n$, situated near a manifold \mathcal{M} in \mathbb{R}^n , such that their sizes obey the constraint $I \leq J$, denote $\nu = \lfloor \frac{J}{I} \rfloor$. Then we*

say that the radius that guarantees approximately ν points from P in the support of each point q_i is $\widehat{h}_0 = c_1 h_0$, with c_1 given by

$$\widehat{h}_0 = c_1 h_0, \text{ with } c_1 = \operatorname{argmin}\{c : \#(\bar{B}_{ch_0}(q_i) \cap P) \geq \nu, \forall q_i \in Q\}. \quad (9)$$

Remark 2.2. Let σ be the variance of the Gaussian $w(r) = \exp\{-r^2/\sigma^2\}$. For the normal distribution, four standard deviations away from the mean account for 99.99% of the set. In our case, by the definition of $w_{i,k}$, since h is the square root of the variance, $4\sigma = 4\frac{h}{\sqrt{2}} = 2\sqrt{2}h_1$ covers 99.99% of the support size of $w_{i,k}$.

The following theorem, proved in [14], indicates how the parameters h_1 and h_2 should be selected.

Theorem 2.3. *Let \mathcal{M} be a d -dimensional manifold in \mathbb{R}^n . Suppose given two point-clouds, $P = \{p_j\}_{j=1}^J \subset \mathbb{R}^n$ and $Q = \{q_i\}_{i=1}^I \subset \mathbb{R}^n$, situated near \mathcal{M} , such that their sizes obey the constraint $I \leq J$, and let $\nu = \lfloor \frac{J}{I} \rfloor$. Let $w_{i,j}$ be the locally supported weight function given by $w_{i,j} = \exp\{-\|q_i - p_j\|^2/h^2\}$. Then a neighborhood size of $h = 2\sqrt{2}\widehat{h}_0$ guarantees $2^{1.5d}\nu$ points in the support of $w_{i,j}$, where $\widehat{h}_0 = c_1 h_0$, with c_1 given by (9).*

Theoretical Analysis of the MLOP Method

For the sake of completeness, we mention here several important results regarding the convergence of the MLOP method, its order of approximation, rate of convergence and complexity (for more details, see [14]).

Theorem 2.4 (Convergence to a stationary point). *Let \mathcal{M} be a in \mathbb{R}^n of unknown intrinsic dimension d . Suppose that the scattered data points $P = \{p_j\}_{j=1}^J$ were sampled near the manifold \mathcal{M} , h_1 and h_2 are set as in Theorem 2.3, and the h - ρ set condition is satisfied with respect to \mathcal{M} . Let the points $Q^{(0)} = \{q_i^{(0)}\}_{i=1}^I$ be sampled from P . Then the gradient descent iterations (6) converge almost surely to a local minimizer Q^* .*

Theorem 2.5 (Order of approximation). *Let $P = \{p_j\}_{j=1}^J$ be a set of points that are sampled (without noise) from a d -dimensional C^2 manifold \mathcal{M} , and satisfy the h - ρ condition. Then for a fixed ρ and a finite support of size h of the weight functions $w_{i,j}$, the set Q defined by the MLOP algorithm has an order of approximation $O(h^2)$ to \mathcal{M} .*

Definition 4. *A differentiable function $f(\cdot)$ is called L -smooth if for any x_1, x_2*

$$\|\nabla f(x_1) - \nabla f(x_2)\| \leq L\|x_1 - x_2\|.$$

Theorem 2.6 (Rate of convergence). *Suppose the point-set $P = \{p_j\}_{j=1}^J$ is sampled near a d -dimensional manifold in \mathbb{R}^n and the assumptions of Theorem 2.4 are satisfied. Suppose the cost function G defined in (1) is an L -smooth function. For $\epsilon > 0$, let Q^* be a local fixed-point solution of the gradient descent iterations, with step size $\gamma = \epsilon^{-1}$. Set the termination condition as $\|\nabla f(x)\| \leq \epsilon$. Then Q^* is an ϵ -first-order stationary point that will be reached after $k = L(G(Q^{(0)}) - G(Q^*))\epsilon^{-2}$ iterations, where $L = l^2$ and $l < \infty$ is a bounded parameter.*

Theorem 2.7 (Complexity). *Given a point-set $P = \{p_j\}_{j=1}^J$ sampled near a d -dimensional manifold $\mathcal{M} \in \mathbb{R}^n$, let $Q = \{q_i\}_{i=1}^I$ be a set of points that will provide the desired manifold reconstruction. Then the complexity of the MLOP algorithm is $O(nmJ + kI(nm\widehat{I} + \widehat{J}))$, where the number of iterations k is bounded as in Theorem 2.6, $m \ll n$ is the smaller dimension*

to which we reduce the dimension of the data, and \widehat{I} and \widehat{J} are the numbers of points in the support of the weight functions $\widehat{w}_{i,v}$, $w_{i,j}$ that belong to the Q -set and P -set, respectively. Thus, the approximation is linear in the ambient dimension n , and does not depend on the intrinsic dimension d .

2.2 Preliminaries — Radial Basis Functions

Radial Basis Functions constitute a very useful and convenient multivariate interpolation tool [6, 13]. Given the values of a function $f : \mathbb{R}^n \rightarrow \mathbb{R}^s$ at center points $x_i \in \mathbb{R}^n$, $i = 1, \dots, K$, we approximate the value of f at a new point x by the formula

$$\widetilde{f}(x) = \sum_{i=1}^K \lambda_i \phi(\|x - x_i\|), \quad (10)$$

where $\phi : \mathbb{R}_+ \rightarrow \mathbb{R}$ is a radial basis function and λ_i are scalar parameters chosen to maintain interpolation at the center points, i.e., $\widetilde{f}(x_i) = f(x_i)$. For examples of possible choices of radial basis functions, see [7, 30]. In the numerical examples presented below we choose to use the following Gaussian RBF with local support:

$$\begin{aligned} \phi_1(r) &= \exp\{-(r/h)^2\}, \\ \phi_2(r) &= \exp\{-(r/h)^2\}(1 + r/h), \\ \phi_3(r) &= \exp\{-(r/h)^2\}(15 + 15(r/h) + 6(r/h)^2 + (r/h)^3). \end{aligned}$$

In what follows, we will state a theorem proved in [31] on the order of approximation in a Sobolev space of a method that uses a RBF of general form, namely

$$\widetilde{f}(x) = \sum_{j=1}^K \lambda_j \phi_w(\|x - x_j\|) + \sum_{i=1}^I \alpha_i p_i(x), \quad (11)$$

where $\phi_w := \phi(\cdot/w)$, with w depending on the fill-distance h of the points $X = \{x_j\}_{j=1}^K$, p_1, \dots, p_I is a polynomial basis for Π_m (the space of polynomials of degree $\leq m$), and the coefficients λ_j and α_j are chosen to satisfy the linear system $\widehat{f}(x_j) = f(x_j)$ for $j = 1, \dots, K$ and $\sum_{j=1}^K \lambda_j p_i(x_j) = 0$, $i = 1, \dots, I$.

To state the theorem on the order of approximation of the RBF method we need some additional definitions.

Definition 5. For $k \in \mathbb{N}$ p , the Sobolev space $W_p^k(\Omega)$ is defined as

$$W_p^k(\Omega) := \left\{ f : \|f\|_{k, L_p(\Omega)} := \left(\sum_{|\alpha| \leq k} \|D^\alpha f\|_{L_p(\Omega)}^p \right)^{1/p} < \infty \right\}, \quad (12)$$

for $p < \infty$, and as

$$W_\infty^k(\Omega) := \left\{ f : \|f\|_{k, L_\infty(\Omega)} := \sum_{|\alpha| \leq k} \|D^\alpha f\|_{L_\infty(\Omega)} < \infty \right\}, \quad (12')$$

for $p = \infty$.

Definition 6. Let $X = \{x_j\}_{j=1}^K$ be a set of points with fill-distance h and separation distance $\delta = \min_{1 \leq i \neq j \leq N} \|x_i - x_j\|/2$. Then we say that X is quasi-uniformly distributed if there exists a constant $\eta > 0$ independent of X such that

$$2\delta \leq h \leq \eta\delta. \quad (12)$$

Definition 7. Let ϕ_w be a radial basis function, and let $\widehat{\phi}_w$ be its Fourier transforms. Define the supremum of the norm of $\widehat{\phi}_w$ as

$$M_{\phi,w}(r) := \sup_{\theta \in B(0,r)} \|\widehat{\phi}_w(\theta)\|^{-1/2}. \quad (13)$$

Definition 8. Let f be as defined in (11), and ϕ_w be a radial basis function. Then the norm of the corresponding error functional is defined as

$$P_{\phi,X}(x) = \sup_{\|f\|_{\phi} \neq 0} \frac{\|f(x) - \widetilde{f}(x)\|}{\|f\|_{\phi}}, \quad \text{where } \|f\|_{\phi} = \int_{\mathbb{R}^d} \frac{\|\widehat{f}(\theta)\|^2}{\widehat{\phi}_w(\theta)} d\theta. \quad (14)$$

Finally, we are ready to state the promised theorem, proven in [31]

Theorem 2.8. Let $X = \{x_j\}_{j=1}^K$ be a set of quasi-uniformly distributed scattered points (see Definition 6), and let $\widetilde{f}(x)$, defined as in (10), be an interpolant to f on X using the radial basis function $\phi_w = \phi(\cdot/w)$. Let $M_{\phi,w}(r)$ with $r > 0$, be defined as in (13). Assume that there exists a constant $\delta_0 > 0$ such that

$$P_{\phi,X/w}(x/w)M_{\phi,w}(\delta_0/h) \leq o(h^k). \quad (15)$$

Then, for every function $f \in W_{\infty}^k(\Omega)$, with $k \in \mathbb{N}$, the error of the RBF method is estimated as

$$\|f - \widetilde{f}\|_{L_{\infty}(\Omega)} = o(h^k). \quad (16)$$

Remark 2.9. As a result, an important key advantage of the RBF method is that it performs better on quasi-uniform samples. This property will be utilized in the next section.

We will also give a short introduction to the Locally Weighted Average Approximation, which will be used as a reference in the section devoted to our numerical examples. Given the values of the function $f : \mathbb{R}^n \rightarrow \mathbb{R}^s$ at the points $x_i \in \mathbb{R}^n$, the locally weighted average approximation of f at a point x is defined as

$$f(x) = \frac{\sum_i w_i f(x_i)}{\sum_i w_i},$$

where $w_i = \exp\{-\|x_i - x\|^2/h^2\}$, and h is the fill-distance of the points $\{x_i\}_{i=1}^I$. Concerning the accuracy of the method, we note that the locally weighted average approximation reconstructs constant functions.

3 Extending the MLOP Method to Approximation of Functions on a Manifold

Let \mathcal{M} be a smooth d -dimensional manifold in \mathbb{R}^n , where $d \ll n$. Let $P = \{p_j\}_{j=1}^J$ be a set of points which were sampled from \mathcal{M} and are affected by noise, and let $f : \mathcal{M} \rightarrow \mathbb{R}^s$ be a smooth

function. Given noisy measurements of f at the points in P , the approximation problem has two steps:

1. Find a noise-free representation of the manifold \mathcal{M} and the noise-free values of f .
2. Estimate the value of the function f at a new given point x .

Our solution for the first step is based on generalizing the MLOP method designed for manifold denoising to the case of function denoising. The key idea of the solution is to embed the approximation problem in a higher-dimensional space, and denoise the data there. Given the input data, which consists of the set of points $\{p_j\}_{j=1}^J \subset \mathbb{R}^n$ and the set of values $\{f(p_j)\}_{j=1}^J \subset \mathbb{R}^s$, we define a new point-set $\widehat{P} = \{\widehat{p}_j\}_{j=1}^J$ to be the graph of a function f , i.e. as the set of ordered pairs, where $\widehat{p}_j = (p_j, f(p_j))$ is the pairing of p_j with the value $f(p_j)$. The points in \widehat{P} are now considered as data points in \mathbb{R}^{n+s} , taken from the $\widehat{\mathcal{M}} = \text{Graph } f = \{(x, f(x)) : x \in \mathcal{M}\}$. The newly defined set $\widehat{\mathcal{M}}$, being the graph of a smooth function f defined on a smooth d -dimensional manifold, is itself a smooth d -dimensional manifold. It should be noted that prior to the embedding in the $(n+s)$ -dimensional space, the values of f should be normalized to the maximum value of the p_j coordinates, in order to avoid them dominating the p_j entries during the norm calculations of the MLOP algorithm.

In this setting, we are now denoising a d -dimensional manifold embedded in $n+s$ dimensions. We apply the MLOP method on the new data set \widehat{P} , and look for a clean dataset $\widehat{Q} = \{\widehat{q}_i\}_{i=1}^I \subset \mathbb{R}^{n+s}$ which will serve as a noise-free approximation of $\widehat{\mathcal{M}}$. The main advantage of this approach is that with a single MLOP execution on the $\{\widehat{p}_j = (p_j, f(p_j))\}$ data in \mathbb{R}^{n+s} we produce a noise-free set $\widehat{Q} \subset \mathbb{R}^{n+s}$, which in fact consist of a noise-free set Q , that reconstructs the manifold \mathcal{M} , and an estimate of the clean value of the function evaluated at these points, $\widetilde{f}(Q)$.

In the second step, we address the problem of evaluating the function at a new point $z \in \mathcal{M}$. The outcome of the first step is a set of points which is not only noise-free, but also quasi-uniformly distributed on the manifold $\widehat{\mathcal{M}}$. This key idea paves the way towards estimating the value of the function at a new given point on \mathcal{M} , or near \mathcal{M} , with a good order of approximation. Our solution is based on utilizing the RBF approximation, as defined in (10), while setting the centers at the cleaned points Q and appending the corresponding cleaned function values $\widetilde{f}(Q)$. These steps are summarized in Algorithm 1:

Algorithm 1 Function Approximation on a Manifold in High Dimensions

- 1: **Input:** $P = \{p_j\}_{j=1}^J \subset \mathbb{R}^n, \{f(p_j)\}, \{z_k\}_{k=1}^K$ ▷ where $\{z_k\}_{k=1}^K$ is a set of new points for function approximation
 - 2: **Output:** $Q = \{q_i\}_{i=1}^I \subset \mathbb{R}^n, \widetilde{f}(Q), \{\widetilde{f}(z_k)\}_{k=1}^K$
 - 3: Denoise the input data by running MLOP with $\widehat{P} = (P, f(P)) \subset \mathbb{R}^{n+s} \rightarrow \widehat{Q} = (Q, \widetilde{f}(Q))$
 - 4: **for** each $z_k \in \{z_k\}_{k=1}^K$ **do**
 - 5: Approximate $f(z_k)$ via RBF, with centers set at Q and the corresponding $\widetilde{f}(Q)$ values
 - 6: **end for**
-

4 Theoretical Analysis of the Method

In this section we discuss some of the theoretical aspects of the proposed approach to approximation of functions. Our analysis relies on the theory of the MLOP method as well as the RBF

method. Specifically, we can use Theorems 2.4, 2.5, 2.6, 2.7 regarding the convergence of the MLOP algorithm to a stationary point, its rate of convergence, and its complexity, estimated for the problem at hand. We also build on the results about the order of approximation of the MLOP. Thus, we can state the following theorem on the order of approximation for the our approximation problem.

4.1 Order of Approximation

Theorem 4.1 (Order of approximation). *Let $P = \{p_j\}_{j=1}^J$ be a set of points sampled from a d -dimensional C^2 manifold \mathcal{M} without noise that satisfy the h - ρ condition. Let $f : \mathcal{M} \rightarrow \mathbb{R}^s$ be a smooth multivariate function given at points of P . Suppose that $f \in W_\infty^k(\Omega)$ and fulfills all the conditions of Theorem 2.8. Then:*

- (i) *For fixed ρ and δ , there is a set of points $Q = \{q_i\}_{i=1}^I \subset \mathbb{R}^n$ which approximates \mathcal{M} with order $O(\widehat{h}^2)$, where $\widehat{h} = \max\{\widehat{h}_1, \widehat{h}_2\}$ and \widehat{h}_1 and \widehat{h}_2 are as in Definition 3 with respect to the high-dimensional data $\widehat{P} = \{(p_j, f(p_j))\} \subset \mathbb{R}^{n+s}$. Moreover, the order of approximation of f on the set Q is also $O(\widehat{h}^2)$.*
- (ii) *The order of approximation of f at a new point is less than $C_1\widehat{h}^2 + C_2h_2^k$ when using the RBF approximation with centers at Q , and $\tilde{f}(Q)$, where h_2 is the optimal support of $\widehat{w}_{i,i'}$ as in Definition 3, and C_1 and C_2 are constants.*

Proof. Given the input data, which consists of the points $\{p_j\}_{j=1}^J$ and the function values $\{f(p_j)\}_{j=1}^J$, we define a new point-set, which is the graph of the function f , $\widehat{P} = \{\widehat{p}_j\}_{j=1}^J$ sampled from a new manifold $\widehat{\mathcal{M}} \in \mathbb{R}^{n+s}$, where \widehat{p}_j are defined as the pairing of the p_j -data with the corresponding values $f(p_j)$. In this setting, we use the MLOP algorithm to denoise a d -dimensional manifold embedded in $(n+s)$ -dimension. Thus, by applying the MLOP method to the new data we obtain the set \widehat{Q} of points that reconstruct $\widehat{\mathcal{M}}$. From Theorem 2.5 it follows that \widehat{Q} approximates $\widehat{\mathcal{M}}$ with the order $O(\widehat{h}^2)$, where \widehat{h} is the representative distance introduced in Definition 3 for the extended data set $\widehat{P} = \{(p_j, f(p_j))\} \in \mathbb{R}^{n+s}$. Recall that \widehat{Q} is in fact a combination of a noise-free set Q , which reconstructs the manifold \mathcal{M} , and an estimate of the clean values of the function at these points in Q , $\tilde{f}(Q)$. Therefore, the order of approximation of Q to \mathcal{M} , and of the estimated values \tilde{f} to f is $O(\widehat{h}^2)$.

Subsequently, we use an RBF approximation with theoretical order of approximation $O(h^k)$ (as stated in Theorem 2.8). In our case the relevant h is h_2 , the support size of $\widehat{w}_{i,i'}$ as in Definition 3. Therefore, the overall order of approximation for a new point is a combination of the two orders, namely $\leq C_1\widehat{h}^2 + C_2h_2^k$, with C_1 , and C_2 constants. \square

4.2 Complexity of the Approximation of Functions

Theorem 4.2. *Let $P = \{p_j\}_{j=1}^J$ be a set of points sampled near a d -dimensional manifold $\mathcal{M} \subset \mathbb{R}^n$ and let $Q = \{q_i\}_{i=1}^I$ be a set of points which will provide the desired noise-free manifold reconstruction. Let $f : \mathcal{M} \rightarrow \mathbb{R}^s$ be a multivariate function given at the points of P . Then the complexity of the approximation of f via the MLOP algorithm for the denoising step is $O((n+s)mJ + kI((n+s)m\widehat{I} + \widehat{J}) + nmI + I\log^2s)$, and for evaluating f at a new point is $O(nm + I)$, where the number of iterations k is bounded as in Theorem 2.6, m , with $m \ll n$, is the smaller dimension to which we reduce the dimension of the data, and \widehat{I} and \widehat{J} are the*

numbers of Q -points and P -points, respectively, in the support of the weight function $\hat{w}_{i,j}$ and $w_{i,j}$.

Proof. The estimate of the complexity of the algorithm can be separated into two steps: **pre-processing** and **evaluating the function at a new point**. The pre-processing step consists of applying the MLOP algorithm in \mathbb{R}^{n+s} , as well as finding the RBF coefficients λ_i by solving the Least-Squares problem. By Theorem 2.7, the complexity of applying the MLOP in the higher dimension $n + s$ is $O((n + s)mJ + kI((n + s)m\hat{I} + \hat{J}))$. The output of this stage is a points set Q of size I , and the corresponding set of values $\tilde{f}(Q)$. From this point on, all the approximation operations are performed on Q , and if $I \ll J$ then we can increase sufficiently the efficiency. The next part of the pre-processing step is to evaluate the radial basis function ϕ for each $q_i \in Q$, which costs $O(nmI)$, and then to find the λ_i by solving the Least-Squares problem, which takes $O(I \log_2^2 s)$ (as shown in [20]). As a result, the complexity of the pre-processing step is $O((n + s)mJ + kI((n + s)m\hat{I} + \hat{J}) + nmI + I \log_2^2 s)$.

Finally, using the λ_i already found, we evaluate the function at a new point in time $O(nm + I)$. It should be stressed that although the pre-processing steps are cost-effective, they are executed once before the function is approximated at a new points set. Thus, if the number of new points for which the approximation needs to be found is large, then the pre-processing steps have less effect on the runtime. \square

5 Numerical Examples

In what follows we present several numerical experiments to demonstrate the advantages of our methodology. We can point out two strengths of the proposed approximation approach. On the one hand, denoising the data domain as well as the function codomain plays an important role in the approximation of functions. On the other hand, sampling the manifold quasi-uniformly improves significantly the approximation of functions by means of classical approximation methods on new data.

Given data sampled from a manifold with noise, and the noisy values of a function f at these points, we follow the function approximation procedure described above. Specifically, we define a new problem in \mathbb{R}^{n+s} , and apply k MLOP iterations to clean the newly defined manifold, which results in a new point-set $Q^{(k)}$, and the corresponding cleaned value set $\tilde{f}(Q^{(k)})$. Next, we randomly select 100 points, $\{z_i\}_{i=1}^{100}$, from a clean reference dataset, and estimate the values of the function f at these points using both the RBF approximation, where the centers of the RBF function are taken at the points of $Q^{(k)}$ (with the radial basis function set to either ϕ_1 , ϕ_2 , or ϕ_3 , as defined below equation (10)), and the locally weighted average approximation (defined by formula 17). As a result, the approximation at the new points relies on the clean quasi-uniformly distributed $Q^{(k)}$ points, as well as on the clean values $\tilde{f}(Q^{(k)})$. In all the stages above we evaluate the accuracy of the approximation as the relative maximum error of the L_1 norm of the difference between the value of \tilde{f} at the new point and the value of f at the closest point in the reference dataset, as well as the root-mean-square error and the standard deviation.

We start with two examples of functions, one smooth and the other non-smooth, both on a one-dimensional manifold embedded in a high-dimensional space. Although in principle the approximation requires a smooth function, it can still be applied to a non-smooth function, provided that we end up with a smoothed result. Specifically, we consider the case of the manifold $O(2)$ of orthogonal matrices, embedded in a 60-dimensional linear space by using the

parameterization

$$p = [\cos(\theta), -\sin(\theta), \sin(\theta), \cos(\theta), 0, \dots, 0], \quad (17)$$

where $\theta \in [-\pi, \pi]$. The input dataset \widehat{P} was constructed by sampling 500 equally distributed points in the parameter space. Next, we randomly sampled an orthogonal matrix $A \in \mathbb{R}^{60 \times 60}$, and created a new point-set via the non-trivial vector embedding

$$P = A\widehat{P}. \quad (18)$$

Subsequently, we added a uniform noise $U(-0.1, 0.1)$, and initialized the set Q by selecting 55 points from P . Figure 1 (A) illustrates the first two coordinates of the points in our set (after multiplication by the matrix A^{-1}). The noisy sample points are shown in green, while the initial reconstruction points are shown in red.

We start by approximating the **smooth function** $f(x) = \frac{1}{4}(1 + \sin(10\theta))$, where θ corresponds to the value used in the expression (17) of p . Next, a uniform noise $U(-0.1, 0.1)$ was added in the codomain (see Figure 1 (C)), and then we applied the MLOP algorithm, which reconstructed the manifold (Figure 1 (B)), as well as denoised function values (Figure 1 (D)). Table 1 summarizes the errors that correspond to different scenarios. We first notice that due to the denoising effect on Q points the maximum relative error decreased from 0.31 to 0.13 for noisy data $Q^{(0)}$ as opposed to the clean data $Q^{(150)}$. Next, we can also see the benefits of using the MLOP algorithm prior to approximating the function with the RBF method on the new data. In the present example the maximum relative error of the best RBF execution decreased dramatically from 0.66 when running the RBF with centers at $Q^{(0)}$, to an 0.12 when running on the quasi-uniform data, and with very low error variance. A quick comparison between the RBF method and the approximation via locally weighted average shows that the latter loses the battle to RBF (even though it produce better results on the clean data versus the noisy one).

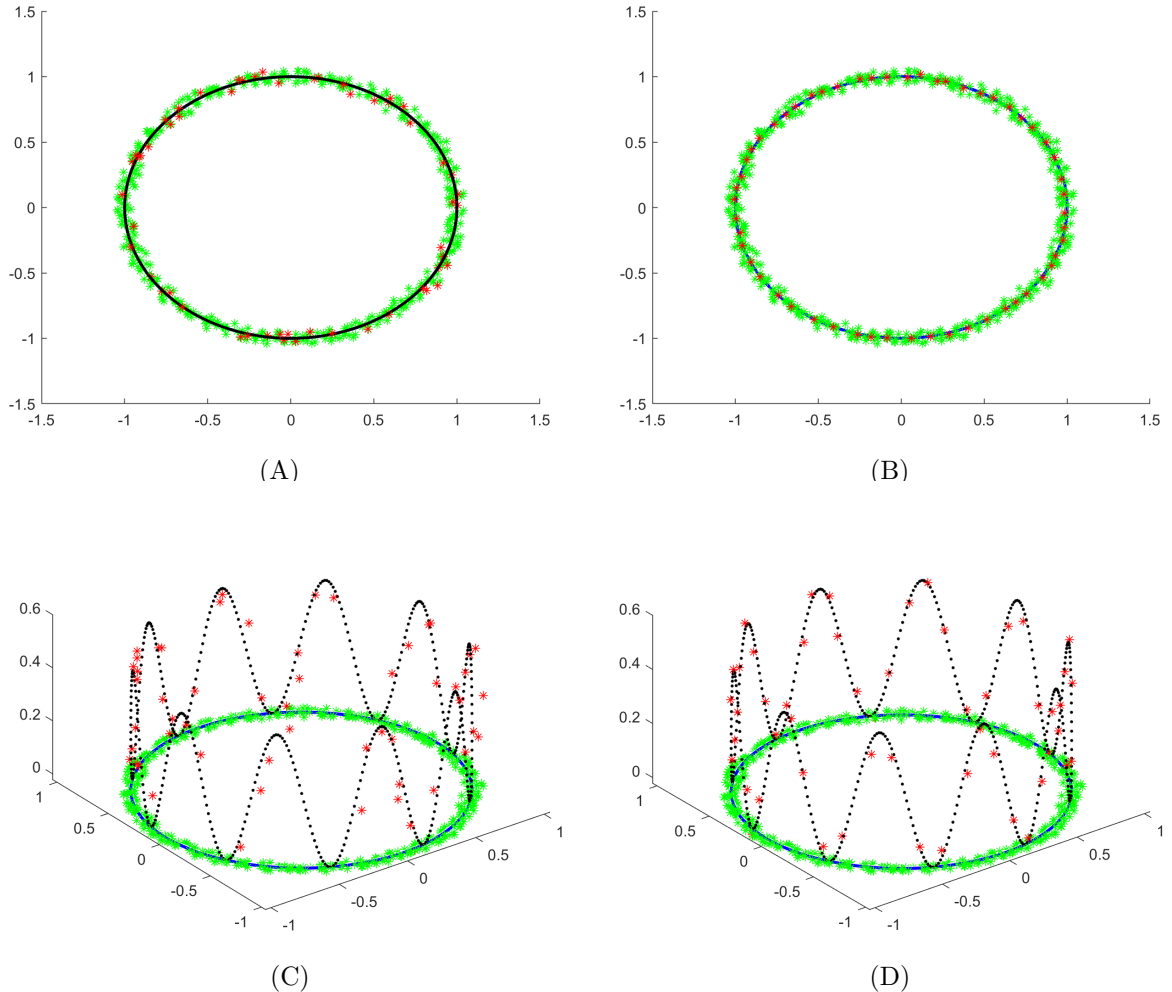


Figure 1: Manifold of orthogonal matrices embedded in a 60-dimensional space. Shown are the first two coordinates of the point-set (after multiplication by A^{-1}). (A) Scattered data with uniformly distributed noise $U(-0.1; 0.1)$ (green), and the initial point-set $Q^{(0)}$ (red). (B) The resulting point-set of the MLOP algorithm after 150 iterations, $Q^{(150)}$ (red), overlaying the noisy samples (green). (C) The initial function values evaluated at the original point-set $Q^{(0)}$ with noise $U(-0.1, 0.1)$. The black line shows the noise-free reference data. (D) Smooth function approximation via the MLOP algorithm at the data points $Q^{(150)}$.

We then applied the approximation procedure to the **non-smooth** function given by $f(x) = \frac{1}{6}(1 + \arccos(\cos(10\theta)))$. We evaluated the function at the P -points and added the uniform noise $U(-0.1, 0.1)$ (see Figure 2 (A)). Then, we applied the MLOP algorithm, which resulted in a reconstructed manifold, as well as denoised function values; see Figure 2 (B). As this figure shows, the non-smooth function f is approximated reliably. This is also reflected in the errors listed in Table 1, which shows that the approximation error decreased from 0.2 to 0.1 after the denoising procedure. The advantages of the MLOP approach are also demonstrated by the error decrease, for the best choice of radial basis function, from 0.77 to 0.15 for approximation on a new point-set. This shows the robustness of the approximation process with respect to the clean data. Here again, we see that the RBF method produces a better approximation than the weighted average.

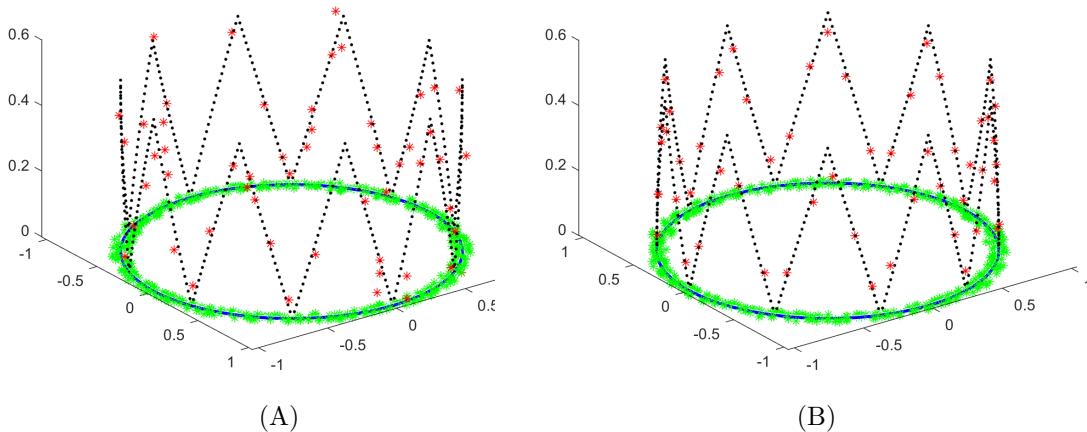


Figure 2: Manifold of orthogonal matrices embedded in a 60-dimensional space. Shown are the first two coordinates of the point-set (after multiplication by A^{-1}). Scattered data with uniformly distributed noise $U(-0.1; 0.1)$ (green), and the Q point-set (red). Left: The initial function values evaluated at the original $Q^{(0)}$ -points with noise $U(-0.1, 0.1)$. The black line shows the noise-free reference data. Right: Approximation of our non-smooth function via MLOP at the data points $Q^{(150)}$.

Table 1: Summary of the maximum and root mean squared errors with standard deviations errors of approximation of functions on the $O(2)$ manifold embedded into 60-dimensional space

	$f(x) = \frac{1}{4}(1 + \sin 10x)$		$f(x) = \frac{1}{6}(1 + \arccos(\cos 10x))$	
	Max relative error	RMSE \pm var	Max relative error	RMSE \pm var
Error over $Q^{(k)}$				
$f(Q^{(0)})$	0.31	0.06 ± 0.0011	0.2	0.04 ± 0.0007
$f(Q^{(150)})$	0.13	0.03 ± 0.0003	0.1	0.03 ± 0.0002
Error over 100 new points				
RBF, ϕ_1 , centers at $Q^{(0)}$, noisy f	0.66	0.14 ± 0.0079	0.77	0.16 ± 0.010
RBF, ϕ_1 , centers at $Q^{(150)}$, cleaned \tilde{f}	0.12	0.03 ± 0.0002	0.15	0.03 ± 0.0004
RBF, ϕ_2 , centers at $Q^{(150)}$, cleaned \tilde{f}	0.12	0.03 ± 0.0002	0.16	0.03 ± 0.0003
RBF, ϕ_3 , centers at $Q^{(150)}$, cleaned \tilde{f}	0.24	0.05 ± 0.0009	0.21	0.05 ± 0.0007
Weighted average	0.28	0.10 ± 0.0018	0.32	0.09 ± 0.0024

In what follows we demonstrate our function approximation methodology on several examples of a low-dimensional manifold embedded in high-dimensional space. Specifically, we embedded a two-dimensional cylindrical structure and then a six-dimensional cylindrical structure in \mathbb{R}^{60} . We start with the two-dimensional cylindrical structure. We sampled the structure using the parameterization

$$p = tv_1 + \frac{R}{\sqrt{2}}(\cos(u)v_2 + \sin(u)v_3),$$

where $v_1 = [1, 1, 1, 1, 1, \dots, 1]$, $v_2 = [0, 1, -1, 0, 0, \dots, 0]$, $v_3 = [1, 0, 0, -1, 0, \dots, 0]$ ($v_1, v_2, v_3 \in \mathbb{R}^{60}$), $t \in [0, 2]$ and $u \in [0.1\pi, 1.5\pi]$. Using this representation, 800 equally distributed (in parameter space) points were sampled with uniformly distributed noise (i.e., $U(-0.1, 0.1)$). We evaluated the function $f(t, u) = 1.3(1 + \sin(0.5u + 1.5t))$ at these points, and constructed the initial Q -set by randomly sampling 150 points (see Figure 3 (A) for the P and Q data, and Figure 3 (C) for the values of the function at the Q -points). The representative distances of the P -set and Q -set were $h_1 = 0.19$ and $h_2 = 0.27$, respectively. Next, we applied the MLOP algorithm on the new data of $(P, f(P))$, and extracted the sets Q and $\tilde{f}(Q)$ (see Figure 3 (B) for the cleaned Q -points, and Figure 3 (D) for the cleaned values at the Q -points). In addition, we approximated the values of f at 100 new points, randomly selected from the reference data. The evaluation error results are summarized in Table 2. The maximum relative L_1 error and the RMSE accompanied with the variance are summarized in Table 2. It should be noted that since we compare the maximum error to clean data, the relative error can exceed 1. One can see that the new data RBF with ϕ_2 as well as ϕ_3 achieve the lowest errors.

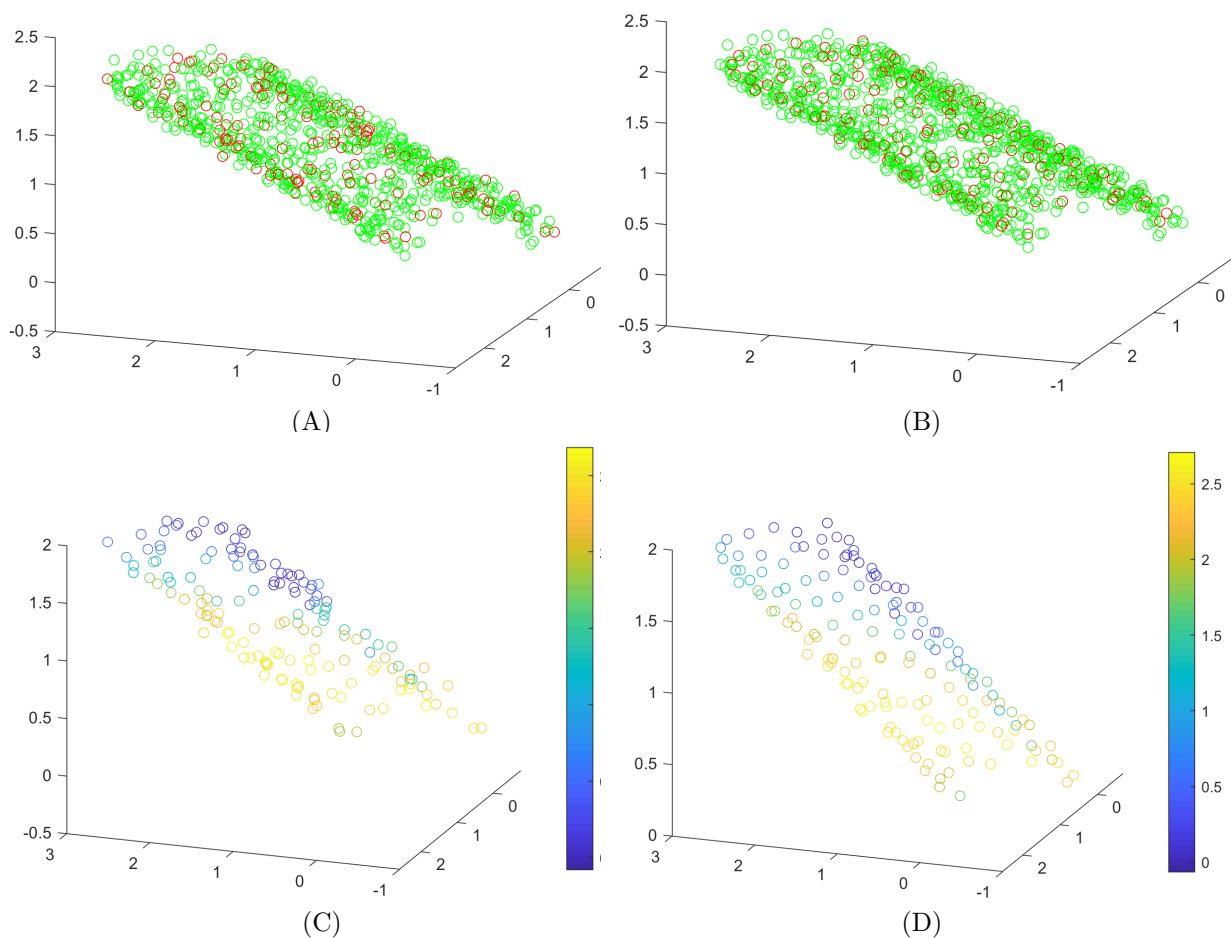


Figure 3: Two-dimensional cylindrical structure embedded in a 60-dimensional space. The first three coordinates of the point-set are shown. (A) Scattered data with uniformly distributed noise $U(-0.1; 0.1)$ (green), and the initial point-set $Q^{(0)}$ (red). (B) The resulting point-set of the MLOP algorithm after 200 iterations, $Q^{(300)}$ (red), overlaying the noisy samples (green). (C) The initial values of the function at the original $Q^{(0)}$ -points with noise $U(-0.1, 0.1)$. (D) MLOP approximation at the data points $Q^{(300)}$.

Six-dimensional cylindrical structure

Next, we tested our method on higher-dimensional manifolds by utilizing an n -sphere to generate an $(n + 1)$ -dimensional cylinder (in the example of the two-dimensional cylinder, we used a circle to generate the structure). Here, we utilized a five-dimensional sphere to build a six-dimensional manifold, using the parameterization

$$x_1 = R \cos(u_1), \quad x_2 = R \sin(u_1) \cos(u_2), \quad \dots, \quad x_6 = R \sin(u_1) \sin(u_2) \cdots \sin(u_5) \sin(u_6).$$

We then embedded the sampled data in a 60-dimensional space by the parametrization

$$p = tv_0 + R^2[x_1, x_2, x_3, x_4, x_5, x_6, 0, \dots, 0], \quad (19)$$

where $R = 1.5$, $t \in [0, 2]$, $u_i \in [0.1\pi, 0.6\pi]$, and $v_0 \in \mathbb{R}^{60}$ is a vector with 1's in positions $1, \dots, d + 1$ and 0 in the remaining positions. We randomly sampled the P -points from the six-dimensional cylindrical structure and embedded the sampled data in a 60-dimensional space. This process resulted in 1200 points in the P -set. We evaluated the function $f(u_1, \dots, u_6) = \sum_{i=1}^6 u_i$ at these points, and constructed the initial Q -set by randomly sampling 460 points. Next, uniformly distributed noise $U(-0.2; 0.2)$ was added to the points. To avoid trying to visualize a six-dimensional manifold, we plot here the cross-section of the cylindrical structure in three dimensions. In Figure 4 (A) we present the P - and Q -data, and in Figure 4 (C) the values of the function at the Q -points. The representative distances of the P -set and Q -set were $h_1 = 0.24$ and $h_2 = 0.37$, respectively. We then applied the MLOP algorithm on the new data of $(P, f(P))$, and extracted the sets Q and $\tilde{f}(Q)$ (see Figure 4 (B) for the cleaned Q -points, and Figure 4 (D) for the cleaned function values at the Q points). In addition, we approximated the values of the function at 100 new points, randomly selected from the reference data. The maximum relative L_1 error and the RMSE accompanied with the variance are summarized in Table 2. One can see that the new data RBF with ϕ_2 and the weighted average achieve lower errors.

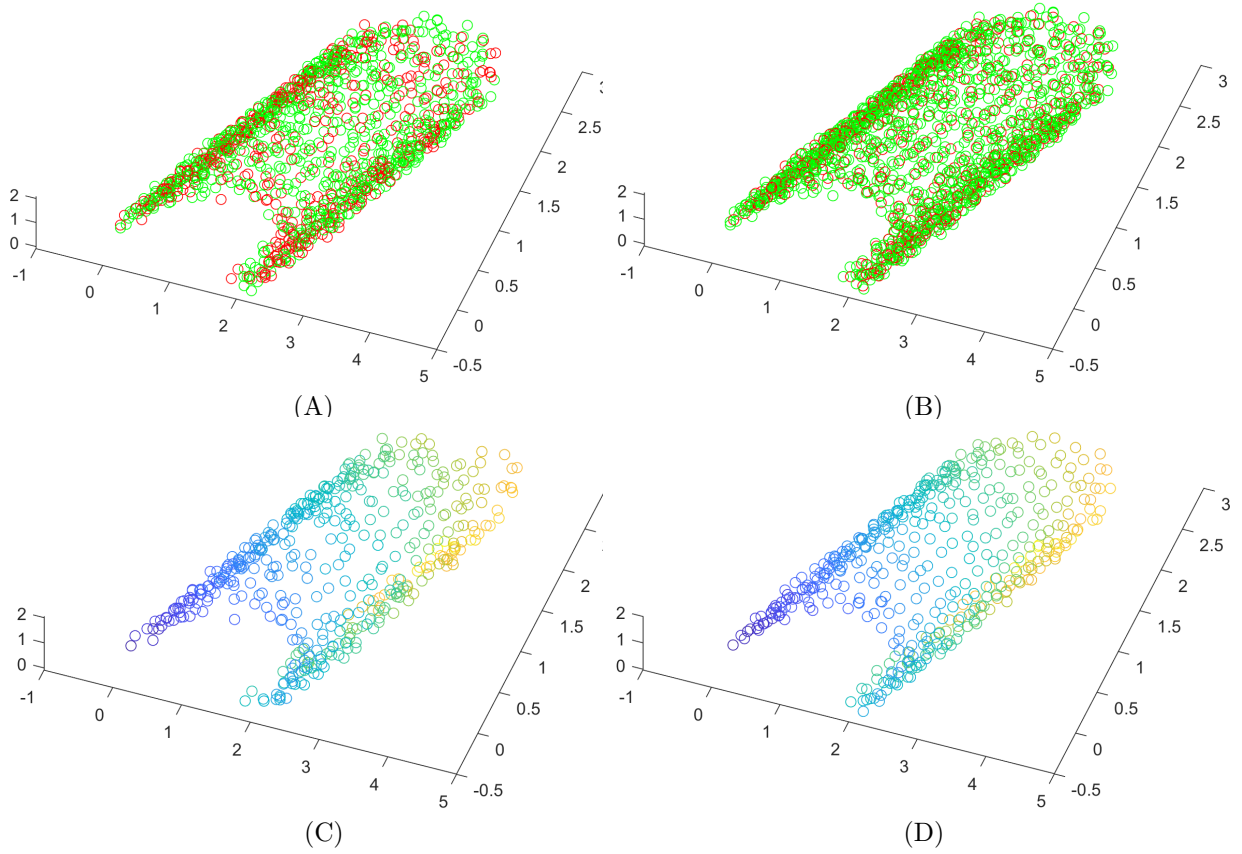


Figure 4: Six-dimensional cylindrical structure embedded in a 60-dimensional space. Plot of the cross-section of the cylindrical structure in three dimensions. (A) Scattered data with uniformly distributed noise $U(-0.2; 0.2)$ (green), and the initial point-set $Q^{(0)}$ (red). (B) The resulting point-set of the MLOP algorithm after 300 iterations, $Q^{(300)}$ (red) overlaying the noisy samples (green). (C) The initial function values evaluated at the original $Q^{(0)}$ points with noise $U(-0.2, 0.2)$. (D) MLOP approximation at the data points $Q^{(300)}$.

Table 2: Summary of the maximum and root mean squared error with standard deviations errors of approximation of a function on a two-dimensional and six-dimensional cylindrical manifold embedded in a 60-dimensional space

	2D cylinder in \mathbb{R}^{60}		6D cylinder in \mathbb{R}^{60}	
	Max relative error	RMSE \pm var	Max relative error	RMSE \pm var
Error over $Q^{(k)}$				
$f(Q^{(0)})$	0.11	0.09 ± 0.0029	0.066	0.08 ± 0.0018
$f(Q^{(300)})$	0.06	0.05 ± 0.0012	0.054	0.06 ± 0.0012
Error over 100 new points				
RBF with ϕ_1 , centers at $Q^{(0)}$, noisy f	1.37	0.3 ± 0.04	0.42	0.4 ± 0.063
RBF with ϕ_1 , centers at $Q^{(300)}$, cleaned \tilde{f}	0.38	0.13 ± 0.007	0.26	0.26 ± 0.026
RBF with ϕ_2 , centers at $Q^{(300)}$, cleaned \tilde{f}	0.11	0.05 ± 0.0009	0.08	0.07 ± 0.0018
RBF with ϕ_3 , centers at $Q^{(300)}$, cleaned \tilde{f}	0.10	0.04 ± 0.0006	0.13	0.04 ± 0.0007
Weighted average	0.2	0.1 ± 0.0024	0.09	0.06 ± 0.0027

Robustness to Noise

In the following example, we examine the effect of the noise level in the target domain on the quality of the approximation. To do this numerically, we sampled a function over a Swiss Roll using the parameterization

$$p = \frac{1}{10}[x, y, z, 0, \dots, 0],$$

where $x = t \sin(t)$, y is a random number in the range $[-6, 6]$, and $z = t \cos(t)$, with $t = 8k/n+2$ and $k \in \mathbb{N}$. The approximated function was $f(p) = t$. We created a Swiss Roll with 800 data points, and randomly sampled 200 points as the initial Q -set. We added noise with various magnitudes (0.1, 0.2, 0.5, and 0.7) to the P -points as well as to the values of f at the P -points. For example, Figure 5 left shows a case of approximation with uniformly distributed noise $U(-0.2, 0.2)$, while the right plot presents the denoised version. We see that the data were cleaned both in the domain and in the codomain of the function. In Figure 6, we plot the error values under various noise scenarios in the codomain, both for the noisy $Q^{(0)}$ data and the error of the RBF approximation on the $Q^{(300)}$ data. One can see that although the approximation error increases on the noisy data (from 0.03 to 0.22), the approximation error on clean and quasi-uniformly distributed data error grows only moderately (from 0.02 to 0.18). We also see that at high levels of noise (e.g., 0.7) the accuracy is good. This shows the strengths of our approach, and justifies the need for data denoising as well as uniform sampling before approximation algorithms are applied.

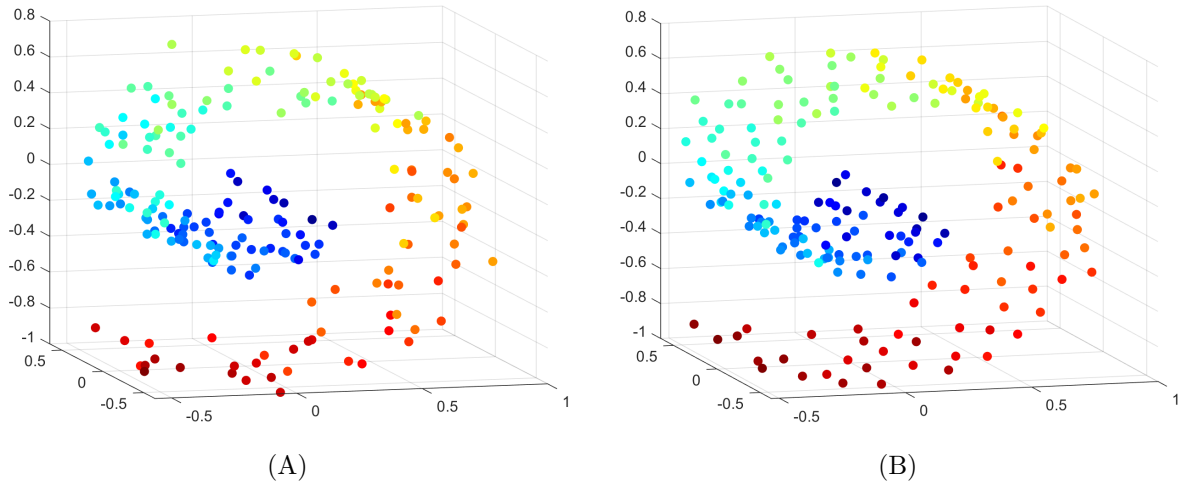


Figure 5: Swiss Roll embedded in \mathbb{R}^{60} . The figure depicts the first three coordinates. Left: The initial values of the function at the original $Q^{(0)}$ points with noise $U(-0.2, 0.2)$, with values indicated by the color. Right: MLOP function approximation at the data points $Q^{(300)}$ cleaned via the MLOP.

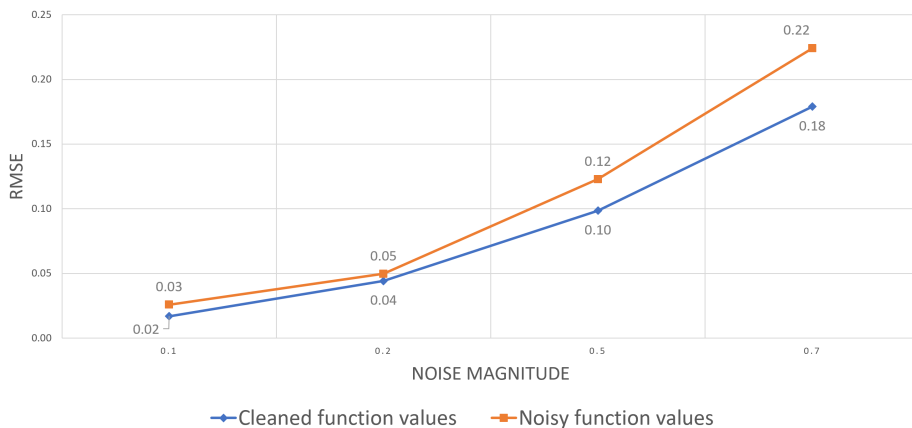


Figure 6: Effect of noise level on the accuracy of function approximation for a Swiss Roll embedded in a 60-dimensional space. The RMSE error evaluated on the original noisy data is shown in orange, while the RMSE error on the cleaned data is presented in blue.

6 Discussion and Conclusions

In this paper, we consider the problem of approximating a function on a manifold in high dimensions, with noise present both in the domain and in the codomain of the function. Given a set of points and the values of an unknown function evaluated at these points, the goal is to find the approximation of the function at a new dataset. While in low dimensions this problem did receive a lot of attention in approximation theory, in high dimensions the solution is challenged by the curse of dimensionality. In our solution, we propose to combine the best of both worlds, the Manifold Locally Optimal Projection (MLOP) [14] and the method of Radial Basis Functions (RBF) methods [13]. The approximation problem has two steps. First, find a noise-free representation of the manifold in terms of new points, and the noise-free values of the function at these points. Then, estimate the value of the function at a new given point

x using the RBF method, with the centers set at the cleaned points. The MLOP method is used here for noise removal and for the generation of a quasi-uniform manifold sampling, as a pre-processing step for the RBF method; this improves the approximation results dramatically. In the paper, we showed that the order of approximation at the new data points is less than $C_1 h^2 + C_2 h_2^k$, where h is the representative distance of the graph of the function f of the initial data, and h_2 is the representative distance of the MLOP reconstruction.

A possible future direction would be to investigate a classification problem. Thus, given data that lies on a manifold, and the corresponding values of a non-smooth function which received only k values, each representing a different class. In addition, both the data and the labeling contain noise and outliers. The research question to be addressed is whether new data can be classified with high accuracy.

An additional possible future direction would be to deal with optimization of functions on a manifold. In the past decade, optimization gained a lot of attention, especially with the rise of Neural Networks computing (NN). Optimization algorithms are the pillar stones of the NNs, as they are in charge of constructing the networks, by learning from the training examples. In our research, we propose introducing a new optimization process, that will take into account the topology of the data. We would like to utilize the manifold structure of the data to improve the optimization process, by incorporating the manifold's information into the NN optimization of a function. We propose extending the MLOP framework to deal with this task, by modifying the definition of the MLOP cost function to include the optimized function. By extending the definition of the MLOP algorithm, the gradient descent iterations will find not only the optimal manifold reconstruction, but also minimize the function.

Acknowledgments

We would like to thank Dr. Barak Sober for valuable discussions and comments. This study was supported by a generous donation from Mr. Jacques Chahine, made through the French Friends of Tel Aviv University, and was partially supported by ISF grant 2062/18.

References

- [1] Amir, A., Levin, D.: High order approximation to non-smooth multivariate functions. *Computer Aided Geometric Design* **63**, 31–65 (2018)
- [2] Andras, P.: High-dimensional function approximation with neural networks for large volumes of data. *IEEE Transactions on Neural Networks and Learning Systems* **29**(2), 500–508 (2017)
- [3] Barzilai, J., Borwein, J.M.: Two-point step size gradient methods. *IMA Journal of Numerical Analysis* **8**(1), 141–148 (1988)
- [4] Bickel, P.J., Li, B., et al.: Local polynomial regression on unknown manifolds. In: *Complex Datasets and Inverse Problems*, pp. 177–186. Institute of Mathematical Statistics (2007)
- [5] Binev, P., Dahmen, W., Lamby, P.: Fast high-dimensional approximation with sparse occupancy trees. *Journal of Computational and Applied Mathematics* **235**(8), 2063–2076 (2011)

- [6] Buhmann, M.D.: Radial Basis Functions: Theory and Implementations, vol. 12. Cambridge University Press, Cambridge Monographs on Applied and Computational Science (2003)
- [7] Buhmann, M.D., De Marchi, S., Perracchione, E.: Analysis of a new class of rational RBF expansions. *IMA Journal of Numerical Analysis* **40**(3), 1972–1993 (2020)
- [8] Chen, M., Jiang, H., Liao, W., Zhao, T.: Efficient approximation of deep ReLU networks for functions on low dimensional manifolds. In: *Advances in Neural Information Processing Systems*, pp. 8174–8184 (2019)
- [9] Coifman, R.R., Lafon, S., Lee, A.B., Maggioni, M., Nadler, B., Warner, F., Zucker, S.W.: Geometric diffusions as a tool for harmonic analysis and structure definition of data: Diffusion maps. *Proceedings of the National Academy of Sciences* **102**(21), 7426–7431 (2005)
- [10] Coifman, R.R., Maggioni, M.: Diffusion wavelets. *Applied and Computational Harmonic Analysis* **21**(1), 53–94 (2006)
- [11] Cox, T.F., Cox, M.A.: *Multidimensional Scaling*. Chapman and Hall, London (2000)
- [12] DeVore, R., Petrova, G., Wojtaszczyk, P.: Approximation of functions of few variables in high dimensions. *Constructive Approximation* **33**(1), 125–143 (2011)
- [13] Dyn, N., Levin, D.: Iterative solution of systems originating from integral equations and surface interpolation. *SIAM Journal on Numerical Analysis* **20**(2), 377–390 (1983)
- [14] Faigenbaum-Golovin, S., Levin, D.: Manifold reconstruction and denoising from scattered data in high dimension via a generalization of l_1 -median (2020)
- [15] Fisher, R.A.: The use of multiple measurements in taxonomic problems. *Annals of Eugenics* **7**(2), 179–188 (1936)
- [16] Grohs, P., Sprechler, M.: Projection-based quasiinterpolation in manifolds. *SAM Report* **23** (2013)
- [17] He, X., Niyogi, P.: Locality preserving projections. In: *Advances in Neural Information Processing Systems*, pp. 153–160 (2004)
- [18] Levin, D.: The approximation power of moving least-squares. *Mathematics of Computation* **67**(224), 1517–1531 (1998)
- [19] Levin, D.: Between moving least-squares and moving least- ℓ_1 . *BIT Numerical Mathematics* **55**(3), 781–796 (2015)
- [20] Li, L.: A new complexity bound for the least-squares problem. *Computers & Mathematics with Applications* **31**(12), 15–16 (1996)
- [21] Lin, T., Zha, H.: Riemannian manifold learning. *IEEE Transactions on Pattern Analysis and Machine Intelligence* **30**(5), 796–809 (2008)
- [22] Lipman, Y., Cohen-Or, D., Levin, D., Tal-Ezer, H.: Parameterization-free projection for geometry reconstruction. In: *ACM Transactions on Graphics (TOG)*, vol. 26, p. 22. ACM

(2007)

- [23] Pearson, K.: LIII. On lines and planes of closest fit to systems of points in space. The London, Edinburgh, and Dublin Philosophical Magazine and Journal of Science **2**(11), 559–572 (1901)
- [24] Roweis, S.T., Saul, L.K.: Nonlinear dimensionality reduction by locally linear embedding. Science **290**(5500), 2323–2326 (2000)
- [25] Shaham, U., Cloninger, A., Coifman, R.R.: Provable approximation properties for deep neural networks. Applied and Computational Harmonic Analysis **44**(3), 537–557 (2018)
- [26] Sober, B., Aizenbud, Y., Levin, D.: Approximation of functions over manifolds: A moving least-squares approach. arXiv preprint arXiv:1711.00765 (2017)
- [27] Tenenbaum, J.B., De Silva, V., Langford, J.C.: A global geometric framework for nonlinear dimensionality reduction. Science **290**(5500), 2319–2323 (2000)
- [28] Vardi, Y., Zhang, C.H.: The multivariate L1-median and associated data depth. Proceedings of the National Academy of Sciences **97**(4), 1423–1426 (2000)
- [29] Woodruff, D.P., et al.: Sketching as a tool for numerical linear algebra. Foundations and Trends in Theoretical Computer Science **10**(1–2), 1–157 (2014)
- [30] Wu, Zong-min., Schaback, R.: Local error estimates for radial basis function interpolation of scattered data. IMA journal of Numerical Analysis **13**(1), 13–27 (1993)
- [31] Yoon, J.: Spectral approximation orders of radial basis function interpolation on the Sobolev space. SIAM Journal on Mathematical Analysis **33**(4), 946–958 (2001)